International Journal of Heat and Mass Transfer 52 (2009) 5330–5338

Contents lists available at ScienceDirect

International Journal of Heat and Mass Transfer

journal homepage: www.elsevier.com/locate/ijhmt

A numerical method for predicting the performance of a randomly packed distillation column

Guo Biao Liu [a,b], K.T. Yu [a], X.G. Yuan [a,*], C.J. Liu [a]

[a] State Key Laboratory for Chemical Engineering and School of Chemical Engineering and Technology, Tianjin University, Tianjin 300072, China
[b] Bayer Technology & Engineering Co., Ltd, Shanghai 201507, China

ARTICLE INFO

Article history:
Received 10 January 2008
Received in revised form 10 June 2009
Accepted 23 June 2009
Available online 21 August 2009

Keywords:
Distillation
Packed column
Simulation
Computational fluid dynamics (CFD)
Diffusivity

ABSTRACT

A numerical method is proposed for modeling the distillation process in a randomly packed column. The proposed model is able to predict the axial and radial concentration distributions along the column without introducing the empirical turbulent Schmidt number or the experimentally measured turbulent mass transfer diffusivity. The present model involves the differential mass transfer equation set and the accompanied computational fluid dynamics (CFD) formulation with the conventional $k-\varepsilon$ model. For the closure of mass transfer equation, the recently developed two-equation model is adopted, which consists of the equations for expressing the fluctuating concentration variance $\overline{c^2}$ and its dissipation rate ε_c [Z.M. Sun, B.T. Liu, X.G. Yuan, C.J. Liu, K.T. Yu, New turbulent model for computational mass transfer and its application to a commercial-scale distillation column, Ind. Eng. Chem. Res. 44 (12) (2005) 4427–4434]. The validity of the proposed model was testified by applying to a commercial scale randomly packed column of 1.22 m internal diameter and packed with 50.8 mm metal Pall rings in 3.66 m bed height for separating cyclohexane/*n*-heptane mixture under total reflux and 165.5 kPa [A. Shariat, J.G. Kunesh, Packing efficiency testing on a commercial scale with good (and not so good) reflux distribution, Ind. Eng. Chem. Res. 34 (4) (1995) 1273–1279]. Satisfactory agreements were found between the model prediction and the published experimental measurement on the axial concentration distributions, the HETP and the turbulent mass transfer diffusivity along the radial and axial directions.

1. Introduction

The packed columns as a kind of phase contractors have been widely used in chemical separation, heat transfer and catalytic reaction processes. Among them, the counter-current operation of gas (vapor) and liquid phases for mass transfer with random packing are frequently employed for distillation and absorption. It is commonly recognized that the rigorous modeling of such column is essential for achieving good design and efficient performance, especially for those of industrial scale, yet the traditional model to be used is based on the assumption of one dimensional flow with axial dispersion. However, due to the non-uniform bed structure and higher porosity in the near wall region of the packed column, the liquid phase behaves not only deviating from one dimensional flow but also displaying complicated dispersion.

The existence of dispersion effect in packed column is one of the main causes to lowering down the column performance and the separation efficiency [3–9] as the concentration gradient and the driving force of mass transfer are being reduced. Many research works regarding this effect have been reported since last five decades [10–19], and summarized in the literature [20].

The dispersion effect, usually represented by a parameter and terminologically denoted by turbulent mass transfer diffusivity or dispersion coefficient, are often evaluated by using either the empirical turbulent Schmidt number Sc_t or the experimental correlation obtained from the tracer experiment [22,23]. Nevertheless, it has been shown that the value of Sc_t is not a constant throughout the whole column as it is affected by both local velocity and concentration [24], and the experimental correlations are mostly formulated by using the one dimensional flow model to fit the experimental data.

One way to overcome this drawback is to closing the differential turbulent mass transfer equation by means of auxiliary equations in order to avoid the direct substation of an empirical diffusivity or experimental coefficient. Recently, Liu et al. [1,25] suggested a $\overline{c^2}-\varepsilon_c$ model for this purpose, in which two auxiliary equations are involved, i.e. the $\overline{c^2}$ equation representing the fluctuating concentration variance and the ε_c equation representing the dissipation rate. This method has been applied successfully for simulating the sieve tray distillation columns [25–27]. In this paper, a numerical method is presented, consisting of the differential mass transfer equation with $\overline{c^2}-\epsilon_c$ closing model and the

* Corresponding author. Tel.: +86 22 27404732; fax: +86 22 27404496.
E-mail address: yuanxg@tju.edu.cn (X.G. Yuan).

0017-9310/$ - see front matter © 2009 Elsevier Ltd. All rights reserved.
doi:10.1016/j.ijheatmasstransfer.2009.06.038

Nomenclature

a	surface area per unit volume of packed bed, m^{-1}
a_e	effective area for mass transfer between the gas phase and liquid phase (m^{-1})
$\overline{c^2}$	concentration variance
$\overline{C}$	average concentration, mass fraction
C_μ, c_1, c_2	model parameters in k-ε model equations
C_{c0}, C_{c1}, C_{c2}, C_{c3}	model parameters in $\overline{c^2}$-ε_c model equations
C_{pk}	characteristic constant of specific type packing
D	molecular diffusivity of C_6 in liquid phase ($m^2\ s^{-1}$)
d_e	equivalent diameter of random packing (m)
d_H	hydraulic diameter of random packing (m)
d_p	nominal diameter of the packed particle (m)
D_{eff}	effective diffusivity, $m^2\ s^{-1}$
D_G	molecular diffusivity of C_6 in gas phase ($m^2\ s^{-1}$)
D_t	turbulent diffusivity for mass transfer ($m^2\ s^{-1}$)
$\mathbf{F}_{LG}$	interface drag force between gas phase and liquid phase ($N\ m^{-3}$)
$\mathbf{F}_{LS}$	flow resistance created by the randomly packing ($N\ m^{-3}$)
F_{pd}	dry packing factor (m^{-1}). For 1/2″(∼1.27 cm) ceramic Berl saddles, F_{pd} = 900 m^{-1}
g	acceleration due to gravity, $m\ s^{-2}$
G	gas phase flow rate per unit cross-section area ($kg\ m^{-2}\ s^{-1}$)
G_f	gas loading factor ($kg\ m^{-2}\ s^{-1}$)
H	volume fraction of liquid phase based on pore space
HETP	height equivalent of theoretical plate
H_{op}	operating holdup
H_s	static holdup
H_t	total liquid holdup
k	turbulent kinetic energy ($m^2\ s^{-2}$)
k_G	gas phase mass transfer coefficient ($kmol\ m^{-2}\ s^{-1}\ kpa^{-1}$)
k_L	liquid phase mass transfer coefficient without chemical reaction ($m\ s^{-1}$)
L	liquid flow rate per unit cross-section area ($kg\ m^{-2}\ s^{-1}$)
L_f	liquid loading factor ($kg\ m^{-2}\ s^{-1}$)
M_A	molecular weight of C_6 ($kg\ kmol^{-1}$)
n-C_7	n-heptane
N_{theo}	number of theoretical stage
p_1, p_2	constants
p_d	period of oscillation normalized by the nominal particle size
p_t	total pressure of gas phase (kPa)
Δp_d	dry-bed pressure drop per meter packing ($N\ m^{-3}$)
Δp_L	wet-bed pressure drop per meter packing, ($N\ m^{-3}$)
Δp_t	total pressure drop per meter packing, ($N\ m^{-3}$)
r	position in radial direction, m
R	radius of the column (m)
R_{e_L}	Reynolds number of liquid phase
R_G	gas universal constant ($kJ\ kmol^{-1}\ K^{-1}$)
S	sink term in concentration equation ($kg\ m^{-3}\ s^{-1}$)
S_{c_t}	Schmidt number
$\mathbf{u}$	interstitial velocity vector of liquid ($m\ s^{-1}$)
$\mathbf{u}_G$	gas velocity vector ($m\ s^{-1}$)
$\mathbf{u}_{slip}$	slip velocity vector between gas phase and liquid phase ($m\ s^{-1}$)
U_L,U_G	liquid and vapor phase superficial velocities, respectively ($m\ s^{-1}$)
x_A	C_6 mole fraction in liquid bulk
$x_{A,I}$	C_6 mole fraction in liquid interface
X_A	C_6 mole concentration in liquid phase ($kmol\ m^{-3}$)
y_A	C_6 mole fraction in gas bulk
$y_{A,I}$	C_6 mole fraction in gas interface
Y_A	C_6 mole concentration in vapor phase ($kmol\ m^{-3}$)
z	axial position
Z	packed-bed height

Greek Symbols

α	relative volatility
ε	turbulent dissipation rate ($m^2\ s^{-3}$)
ε_c	turbulent dissipation rate of concentration fluctuation (s^{-1})
Φ	variable
Φ_L, Φ_G	liquid and gas phase enhancement factors, respectively
γ	porosity distribution of the random packing bed along the radial direction.
γ_∞	porosity in an unbounded packing
μ, μ_t, μ_{eff}	liquid molecular, turbulent and effective viscosity, respectively ($kg\ m^{-1}\ s^{-1}$)
μ_G	gas phase viscosity ($kg\ m^{-1}\ s^{-1}$)
ρ	liquid density ($kg\ m^{-3}$)
ρ_G	gas phase density ($kg\ m^{-3}$)
σ	surface tension of liquid, dynes (cm^{-1} or $N\ m^{-1}$)
σ_c	σ_{ε_c} model parameters in $\overline{c^2}-\varepsilon_c$ model equations
σ_k, σ_ε	model parameters in $k-\varepsilon$ model equations
χ	characteristic length of packing

Subscripts

e	effective
G	gas
I	interface
L	liquid

accompanied computational fluid dynamics (CFD) equations, for the purpose of simulating an industrial scale randomly packed distillation column without introducing the empirical Sc_t number or the experimental correlation. The validity of the proposed model is testified by comparing with the published experimental data [2].

2. The simulated packed column

The industrial scale packed column to be simulated in this paper, as described by Shariat and Kunesh [2], is 1.22 m in diameter and packed randomly with different sizes carbon steel Pall rings (15.9 mm, 25.4 mm, 50.8 mm, and 88.9 mm respectively). The mixture to be separated is cyclohexane/*n-heptane* (C_6/n-C_7), and the separation operation is under total reflux and different pressures (35 kPa and 165.5 kPa). As a tubular drip pan distributor with relatively high drip point density (about 104 points/m^2) is equipped in this column, it could be assumed that the liquid phase at the inlet of packed bed is uniformly distributed. The detailed information about the experimental set-up and operation procedures can be found from the published paper. The physical properties of the separating mixture at 165.5 kPa are listed in Table 1, and some of the published experimental data [2] is given in Tables 2 and 3.

3. Proposed numerical method

3.1. Assumptions

The following assumptions are made for simulating the foregoing described packed column undergoing separation by distillation:

Table 1
The C_6/n-C_7 system physical properties at 165.5 kPa.

System	P (kPa)	ρ_L (kg/m^3)	ρ_G (kg/m^3)	μ_L (Pa·s)	μ_G (Pa·s)	D (m^2/s)	D_G (m^2/s)	σ (N/m)	α
C_6/n-C_7	165.5	636.7	4.907	2.3E-4	8.5E-6	6.2E-9	2.1E-6	0.012	1.6

Table 2
Experimental composition of C_6 at different packed-bed height (50 mm Pall Ring and 165.5 kPa).

Packed-bed height (m)	F-factor [m s^{-1}(kg m^{-3})$^{0.5}$]		
	0.758	1.02	1.52
	Composition of C_6		
0.381	0.2314	0.2314	0.2246
0.991	0.3527	0.3306	0.3114
1.60	0.4576	0.4197	0.4018
2.21	0.6035	0.5881	0.5881
2.819	0.6914	0.6531	0.6385
3.66	0.7857	0.7596	0.7328

Table 3
Experimental HETP (50 mm Pall Ring and 165.5 kPa).

F-factor [m s^{-1}(kg m^{-3})$^{0.5}$]	HETP (m)
0.533	0.758
0.587	1.02
0.584	1.58

(1) The pseudo-single-liquid phase model is applied, i.e. the liquid phase is considered pseudo-continuous, and the gas phase is uniformly distributed along the radial direction. The flow is axially symmetrical.
(2) The distillation operation is in steady state, and the liquid is incompressible. The temperature and density of the liquid phase are considered to be constant as the difference in boiling point and density between hexane and n-heptane are very small.
(3) The constant molar flow is assumed for the gas phase and liquid phase. This assumption is reasonable because the heat of vaporization and condensation of hexane and n-heptane are practically equal.

In addition, as pointed out by Billet [21], the liquid flow in randomly packed column is generally in the turbulent flow region when the liquid Reynolds number Re_L is larger than 10, which is the case often encountered in the industrial operation. Such a condition is applicable to the simulation in this paper.

3.2. Model equations

3.2.1. Mass transfer equation and its auxiliary closing equations

The mass transfer equation expressed in volume average mass fraction $\overline{C}$ of the light component hexane (C_6) in liquid phase is as follows:

$$\nabla\cdot(\rho h\mathbf{u}\overline{C}) = \nabla\cdot(\rho h D_{eff}\nabla\overline{C}) + S \tag{1}$$

where ρ is the liquid density, h is the volume fraction of liquid phase based on pore space, $\mathbf{u}$ is the liquid interstitial velocity vector, S is the sink term accounting for interfacial mass transfer of the component, D_{eff} is the effective mass transfer diffusivity of C_6 in liquid phase and is defined by the following equation:

$$D_{eff} = D + D_t \tag{2}$$

where D is the molecular diffusivity of C_6 in the liquid phase, D_t is the turbulent diffusivity of mass transfer, which can be obtained by applying the $\overline{c^2}-\varepsilon_c$ model [1,25] and expressed as:

$$D_t = C_{c0}k\left(\frac{k}{\varepsilon}\frac{\overline{c^2}}{\varepsilon_c}\right)^{1/2} \tag{3}$$

where the fluctuating concentration variance $\overline{c^2}$ and its dissipation rate ε_c are defined below:

$$\overline{c^2} \equiv \overline{Cc}, \quad \varepsilon_c \equiv D\overline{\left(\frac{\partial c}{\partial x_j}\frac{\partial c}{\partial x_j}\right)} \tag{4}$$

The $\overline{c^2}-\varepsilon_c$ model consists of the following $\overline{c^2}$and ε_c equations:

$$\nabla\cdot(\rho h\mathbf{u}\overline{c^2}) - \nabla\cdot\left[\rho h\left(D+\frac{D_t}{\sigma_c}\right)\nabla\overline{c^2}\right] = 2\rho h D_t\nabla\overline{C}\nabla\overline{C} - 2\rho h\varepsilon_c \tag{5}$$

$$\nabla\cdot(\rho h\mathbf{u}\varepsilon_c) - \nabla\cdot\left[\rho h\left(D+\frac{D_t}{\sigma_{\varepsilon_c}}\right)\nabla\varepsilon_c\right] = C_{c1}h\rho D_t\nabla\overline{C}\nabla\overline{C}\frac{\varepsilon_c}{\overline{c^2}} - C_{c2}\rho h\frac{\varepsilon_c^2}{\overline{c^2}} - C_{c3}\rho h\frac{\varepsilon\varepsilon_c}{k} \tag{6}$$

The constants in Eqs. (5) and (6) are [28]: $C_{c0}=0.11$, $C_{c1}=1.8$, $C_{c2}=2.2$, $C_{c3}=0.8$, $\sigma_c=1.0$ and $\sigma_{\varepsilon_c}=1.0$.

3.2.2. Accompanied CFD equations

As the net quantity in moles of mass transferred between gas phase and liquid phase is zero due to the assumption of constant molar flow, the continuity and momentum equations for the liquid phase flow are as follows:

$$\nabla\cdot(\rho h\mathbf{u}) = 0 \tag{7}$$

$$\nabla\cdot(\rho h\mathbf{u}\mathbf{u}) - \nabla\cdot\left(h\mu_{eff}\left(\nabla\mathbf{u}+(\nabla\mathbf{u})^T\right)\right) = -h\nabla p + \mathbf{F}_{LG} + h(\mathbf{F}_{LS}+\rho\mathbf{g}) \tag{8}$$

$$\mu_{eff} = \mu + \mu_t \tag{9}$$

$$\mu_t = \rho C_\mu\frac{k^2}{\varepsilon} \tag{10}$$

where μ, μ_t and μ_{eff} represent the molecular, turbulent and effective viscosities of the liquid phase, respectively. The turbulent viscosity μ_t is unknown and can be solved simultaneously with the standard $k-\varepsilon$ model as shown below. $\mathbf{F}_{LG}$ is the interface drag force between gas phase and liquid phase, $\mathbf{F}_{LS}$ is the flow resistance, known as the body force resistance, created by the presence of random packing.

The standard $k-\varepsilon$ model consists of the following equations:

$$\nabla\cdot(\rho h\mathbf{u}k) - \nabla\cdot\left[h\left(\mu+\frac{\mu_t}{\sigma_k}\right)\nabla k\right] = h\mu_t\nabla\mathbf{u}\cdot((\nabla\mathbf{u}+(\nabla\mathbf{u})^T)) - \rho h\varepsilon \tag{11}$$

$$\nabla\cdot(\rho h\mathbf{u}\varepsilon) - \nabla\cdot\left[h\left(\mu+\frac{\mu_t}{\sigma_\varepsilon}\right)\nabla\varepsilon\right] = c_1 h\mu_t\nabla\mathbf{u}\cdot\left(\left(\nabla\mathbf{u}+(\nabla\mathbf{u})^T\right)\right)\frac{\varepsilon}{k} - c_2\rho h\frac{\varepsilon^2}{k} \tag{12}$$

The constants in foregoing equations are customarily chosen to be: $C_\mu=0.09$, $\sigma_k=1.0$, $\sigma_\varepsilon=1.3$, $c_1=1.44$ and $c_2=1.92$.

The simultaneous solution of the foregoing mass transfer equation and its auxiliary closing equations together with the accompanied CFD equations is able to give the concentration and the velocity distributions in the distillation column.

3.2.3. Determination of parameters

Before solving the foregoing equation system, the terms of h, S, $\mathbf{F}_{LG}$, and $\mathbf{F}_{LS}$ appeared in foregoing equations must be determined.

The volume fraction h of the liquid phase based on pore space, expressed by $h=H_t/\gamma$, can be determined from the total liquid

holdup H_t and the unevenly distributed porosity γ [4,29,30] under the operating condition concerned. The total liquid holdup H_t is defined as the sum of the static holdup H_s and the operating holdup H_{op}, i.e. $H_t = H_s + H_{op}$. The correlations for estimating H_s, H_{op} and γ are available in the literature [31–33], and those used in this paper are given in the Appendix A.

The interface drag force $\mathbf{F}_{LG}$ is related to the pressure drop caused by the interaction between the liquid and vapor phases. For irrigated packing, the pressure drop Δp_t is greater than that of the dry bed Δp_d due to the presence of liquid adhered to the packing surface and consequently the cross section available for gas flow is reduced. The increased part of pressure drop can be represented by Δp_L, which represents the pressure drop created by the interfacial drag force between gas phase and liquid phase. Then the total pressure drop can be expressed by $\Delta p_t = \Delta p_d + \Delta p_L$. The correlations developed by Robbins [34], as given in the Appendix A, are used to estimate the Δp_d and Δp_L. Finally, the interface drag force $\mathbf{F}_{LG}$ can be expressed by [34]

$$\mathbf{F}_{LG} = \frac{\Delta p_L}{|\mathbf{u}_{slip}|}\mathbf{u}_{slip}$$

where $\mathbf{u}_{slip}$ is the slip velocity between gas phase and liquid phase, which is defined as:

$$\mathbf{u}_{slip} = \mathbf{u}_G - \mathbf{u}$$

The $\mathbf{u}_G$ in axial direction can be determined from gas phase flow rate G.

The liquid flow resistance $\mathbf{F}_{LS}$ created by the presence of random packing can be treated as a body force, and can be calculated by using Ergun equation [35], in which the body force is considered as a nonlinear function of the mean porosity. In the present case, the mean porosity is replaced by the porosity distribution function γ. The relevant equations are given in the Appendix A.

The sink term S, which is the mass of C_6 to be transferred from the liquid phase to the gas phase per unit volume and per unit time, can be determined from the following conventional rate equations:

$$S = k_L a_e M_A X_A (x_A - x_{A,I}) \tag{13}$$
$$S = k_G a_e M_A Y_A (y_{A,I} - y_A) \tag{14}$$

where k_L and k_G are respectively the film coefficients of mass transfer of liquid phase and gas phase, a_e is the effective interfacial area, M_A is the molecular weight of C_6, X_A and Y_A are the mass in mole of C_6 in liquid and vapor phases, $x_{A,I}$ and $y_{A,I}$ are the interfacial concentrations in mole fraction of C_6. Since $x_{A,I}$ and $y_{A,I}$ are in equilibrium at the interface, we have:

$$y_{A,I} = \frac{\alpha x_{A,I}}{1 + (\alpha - 1)x_{A,I}} \tag{15}$$

where α is the relative volatility of the separating mixture. Combining Eqs. (13)–(15), the following equation is obtained:

$$m_0 S^2 + m_1 S + m_2 = 0 \tag{16}$$
$$m_0 = \frac{\alpha - 1}{k_L k_G M_A^2 a_e^2 X_A Y_A} \tag{17}$$
$$m_1 = \frac{(\alpha - 1)y_A - \alpha}{k_L a_e X_A M_A} - \frac{(\alpha - 1)x_A + 1}{k_G a_e Y_A M_A} \tag{18}$$
$$m_2 = \alpha x_A - ((\alpha - 1)x_A + 1)y_A \tag{19}$$

Then, the sink term S can be obtained by solving simultaneously Eqs. (16)–(19). The k_L, k_G and a_e is determined by using the correlations given by Wagner et al. [36], which are listed in the Appendix A.

4. Boundary conditions

The computational domain and boundaries are shown in Fig. 1. The boundary conditions for the modeling equation set are specified as follows:

4.1. Inlet conditions

At the top of the column, the "velocity inlet" boundary is set to be:

$$u = u_{inlet}, \quad v_{inlet} = 0, \quad \overline{C} = \overline{C_{inlet}}, \quad k_{inlet} = 0.003u_{inlet}^2, \quad \varepsilon_{inlet} = 0.09\frac{k_{inlet}^{1.5}}{d_H} \text{ [37]}$$

where d_H denotes the hydraulic diameter of random packing [38], which can be calculated by:

$$d_H = \frac{4\gamma_\infty}{a(1 - \gamma_\infty)}.$$

There are no experimental measurements reported or empirical correlations available from the literature for determining the inlet condition of the concentration variance $\overline{c^2}$ equation. However, according to the experiments for turbulent heat transfer [39–41], and by the analogy between heat and mass transfer, we may assume that:

$$\overline{c_{inlet}^2} = (0.082\overline{C_{inlet}})^2 \tag{20}$$

The boundary condition at the inlet for the ε_c equation is given below [26,27]:

$$\varepsilon_{c,inlet} = 0.4\left(\frac{\varepsilon_{inlet}}{k_{inlet}}\right)\overline{c_{inlet}^2} \tag{21}$$

4.2. Outflow conditions

The flow at the bottom of the column is considered to be close to fully developed, so that the "outflow" boundary condition of zero normal gradients is chosen for all flow variables except pressure.

4.3. Axis conditions

Under the assumption of axial-symmetry, we let $\frac{\partial \Phi}{\partial r} = 0$ at $r = 0$ for all variables Φ.

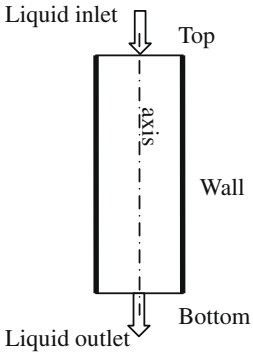

Fig. 1. The simulation domain and boundary conditions arrangement.

4.4. Wall conditions

The no-slip condition is applied to the wall, and the zero flux condition at the wall is adopted, i.e. $\frac{\partial \overline{C_i}}{\partial r} = 0$ at $r = R$ for the mass transfer equation. The conventional logarithm law expression is employed in the near wall region.

5. Numerical procedure

The model equations were solved numerically by using the commercial software FLUENT 6.1 with finite volume method. The well-known SIMPLEC algorithm is used to solve the pressure–velocity coupling problem in the momentum equations. The grid arrangement for the commercial scale column of 3.66 m height and 0.61 m radius is as follows. There are 1000 nodes uniformly distributed along the column height. For the radial direction, total 75 nodes are non-uniformly distributed along the radial direction with higher grid resolution at the near wall region, i.e. 15 nodes are distributed from the wall to the column center by using uniform algorithm to cover radial distance of 0.072 m, in which 0.001 m distance is set between the first row and the wall with growth factor 1.2, then the left 60 nodes are uniformly distributed along the remaining radial distance of 0.538 m. There are about 75,000 quadrilateral cells throughout the column. Such grid resolution is sufficient for the present simulation as illustrated in Section 6.2. The second-order upwind spatial discretization scheme was used for all differential equations.

6. Simulated results and discussion

The simulated results by applying the proposed numerical model are compared with the experimental measurements of a commercial scale distillation column reported by Shariat and Kunesh [2] as given below.

6.1. Radial averaged C_6 concentration profiles along axial direction

The simulated radial concentration is averaged at different height of the column to form the axial concentration along the column. As seen in Fig. 2a–c, the agreement between the model predictions and the experimental data is satisfactory.

6.2. Liquid velocity and concentration profiles

Due to the non-uniform packing structure and higher porosity at the near wall range, the fluid flow can not be uniform. The simulated radial velocity profile is shown in Fig. 3, in which the "wall flow" appears near the wall region, and the flow behaves relatively uniform only about $2d_p$ apart from the wall. This phenomenon has been observed by many investigators [4,33].

The profiles of velocity and the component concentration are shown respectively in Figs. 3 and 4. At a fixed axial position, it is seen that the C_6 concentration increased gradually from the column center to the wall as shown by Fig. 4(e).

To study the effect of grid resolution on the simulated results, the simulation of C_6 concentration profile under F-factor = 1.02 m s^{-1}(kg m^{-3})$^{0.5}$ with higher grid resolution (150 nodes in the radial direction and 1000 nodes in the axial direction) is also conducted as shown in Fig. 4(c). By comparing Fig. 4(b) and (c), no substantial difference is seen, which demonstrates that the grid arrangement with 75 nodes in radial direction and 1000 nodes in axial direction is satisfactory for simulating such an industrial scale column.

6.3. Separation efficiency comparison

The separation efficiency of packed column is usually expressed in terms of height equivalent of theoretical plate (*HETP*). For distillation at total reflux, the HETP may be calculated by the Fenske equation:

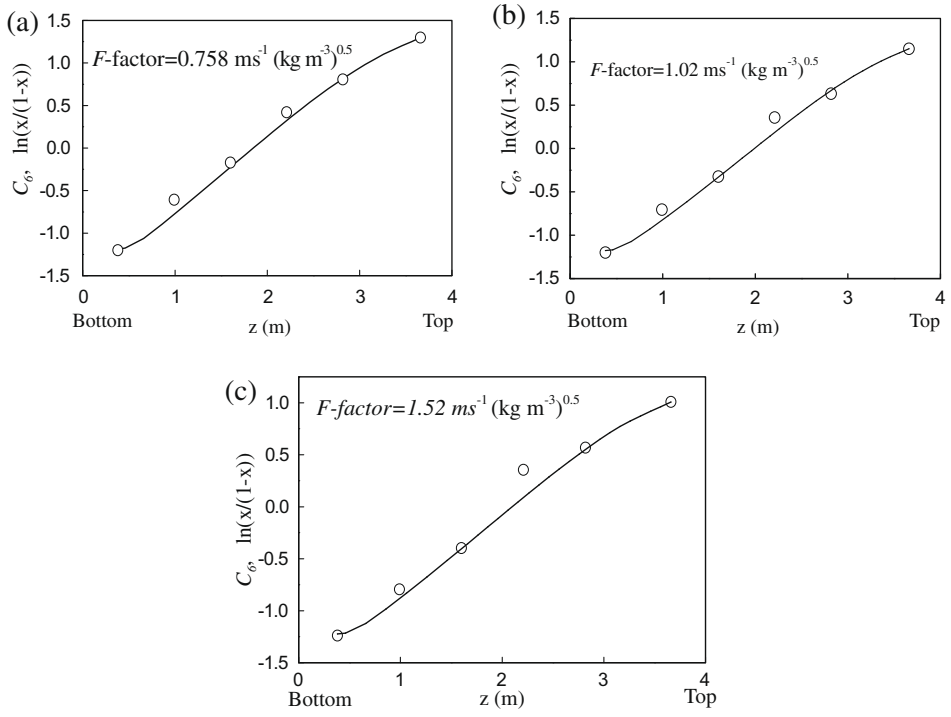

Fig. 2. Comparisons of the concentration profiles in liquid phase between model predictions (solid lines) and experimental measurements (dots) at different F-factors, (a) F-factor = 0.758 m s^{-1}(kg m^{-3})$^{0.5}$, (b) F-factor = 1.02 m s^{-1}(kg m^{-3})$^{0.5}$, (c) F-factor = 1.52 m s^{-1}(kg m^{-3})$^{0.5}$.

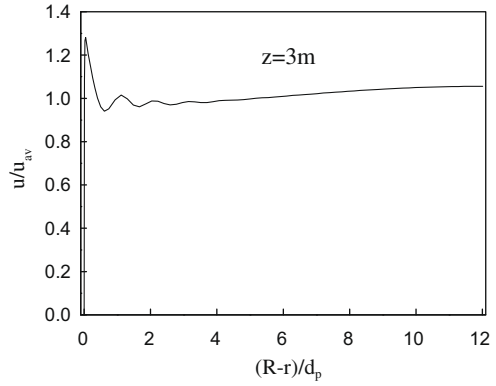

Fig. 3. Relative velocity profile of liquid phase along the radial direction at $z = 3$ m for F-factor = 1.02 m s^{-1}(kg m^{-3})$^{0.5}$.

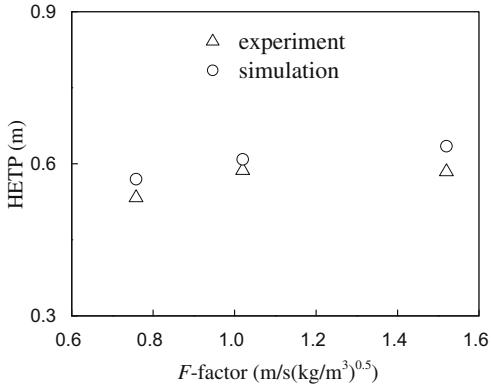

Fig. 5. HETP comparison between prediction and measurements.

$$HETP = Z/N_{theo}$$
$$N_{theo} = \frac{1}{\ln \alpha} \ln\left(\left(\frac{x}{1-x}\right)_{Top}\left(\frac{1-x}{x}\right)_{Bottom}\right) \quad (22)$$

where N_{theo} is the number of theoretical stages, x is the mole fraction of the light component C_6. The simulated and experimentally measured *HETP* values for different *F*-factors are shown in Fig. 5, where the predicted *HETP* values are in reasonable agreement with the experiment, although the former is somewhat higher than the latter.

6.4. Turbulent mass transfer diffusivity D_t

The turbulent diffusivity distribution (D_t profile) along the column can be predicted by means of the present model. To testify the reliability of the prediction, comparisons are made with the

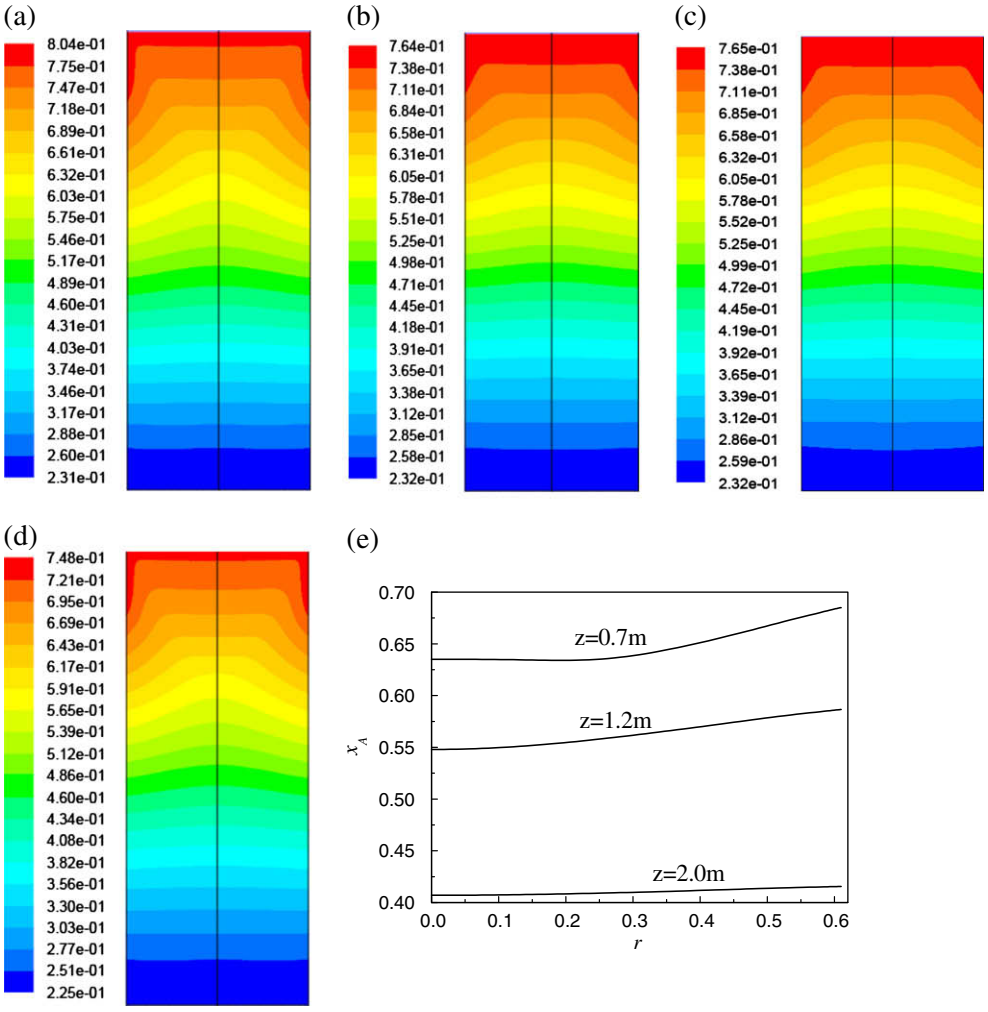

Fig. 4. C_6 Concentration profiles in liquid phase predicted by CMT model at different *F*-factors (a) *F*-factor = 0.758 m s^{-1}(kg m^{-3})$^{0.5}$, (b) *F*-factor = 1.02 m s^{-1}(kg m^{-3})$^{0.5}$ for grid 75 * 1000, (c) *F*-factor = 1.02 m s^{-1}(kg m^{-3})$^{0.5}$ for grid 150 * 1000, (d and e) *F*-factor = 1.52 m s^{-1}(kg m^{-3})$^{0.5}$.

published empirical Schmidt number Sc_t used for packed column and the relevant correlation obtained by using the inert tracer technique. For this purpose, the predicted D_t distribution should be averaged in order to make the comparisons possible.

There are two ways to average the predicted D_t distribution:

(1) Volume average: The average D_t on the volume basis at different height of the packed bed is considered to be the averaged turbulent diffusivity along axial direction, $D_{t,x}$. If the volume refers to the whole column, it is the overall average turbulent diffusivity, $D_{t,av}$.
(2) Radial average: The average D_t at any cross section of the column is considered to be the averaged turbulent diffusivity along radial direction, $D_{t,r}$. It is varying along the column height.

The following are the comparison and discussion:

(1) Michell and Furzer [16] presented a correlation for the dispersion coefficient (turbulent diffusivity) of liquid phase in the packed column in the following form:

$$\frac{|\mathbf{u}|d_p}{D_t} = 1.00\left(\frac{u_{\text{inter}}d_p\rho}{\mu}\right)^{0.7}\left(\frac{d_p^3 g\rho^2}{\mu^2}\right)^{-0.32} \quad (23)$$

Wang et al. [19] correlated the dispersion coefficient with consideration of packing factors as follows:

$$\frac{|\mathbf{u}|d_p}{D_t} = 1.157\left(\frac{U_L d_p\rho}{\mu}\right)^{0.554}\left(\frac{d_p^3 g\rho^2}{\mu^2}\right)^{-0.200}(ad_p)^{-0.190} \quad (24)$$

In Fig. 6, the predicted overall averaged turbulent diffusivity $D_{t,av}$ is compared with the two foregoing correlations of dispersion coefficient at different F-factors. As seen from Fig. 6, the predicted $D_{t,av}$ is in the same order of magnitude with the correlations of dispersion coefficient, although their variation with F-factor shows different tendency.

Ebach and White [14] observed that the axial dispersion is increased with increasing liquid velocity and gas load, while Choe and Lee [10] reported that axial dispersion is decreased with the increase of liquid velocity. In view of different research results, the question that the axial dispersion is increased or decreased with the liquid velocity is not clear, although the influence of liquid velocity on axial dispersion seems small.

(2) The predicted $D_{t,r}$ along the bed length at different F-factors is plotted in Fig. 7. It is seen that $D_{t,r}$ is increasing gradually from the top to the bottom, and also slightly increase at higher F-factor.

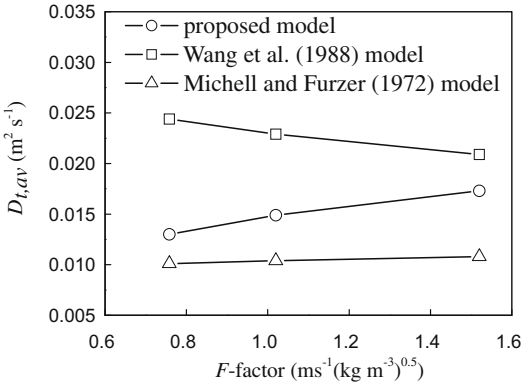

Fig. 6. Comparisons between the predicted volume averaged $D_{t,av}$ and the correlations by Wang et al. [19] and Michell and Furzer [16].

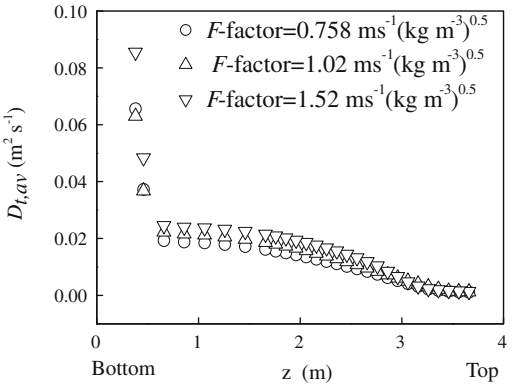

Fig. 7. Predicted $D_{t,r}$ along packed-bed height at different F-factors.

The relationship between $D_{t,r}$ and packed-bed length is also not clear from the existing literature. Ebach and White [14] found no significant effect of bed length on the axial dispersion coefficient. Strang and Geankoplis [12] reported that the axial dispersion was decreased with increasing the bed length due to the end effect. Otake and Kunugita [17] found that the axial dispersion decreased with increasing bed length. Tan and Liou [11] showed that the axial dispersion increased with bed length at the beginning, then kept constant. However, the axial dispersion is not a constant as indicated both by the present simulation and previous researches.

(3) The variations of D_t along radial direction at different axial positions are presented in Fig. 8. Generally, D_t is found to be substantially constant at the bed center because of the relatively uniform velocity and concentration distributions, and reaching a maximum near the column wall due to the wall flow effect, and then decreasing sharply at the wall as a result of the no-slip boundary condition at the wall surface. Such phenomenon is consistent with the experimental results [13,15]. In addition, Fig. 9 shows the contour of turbulent diffusivity D_t along the column.

7. Conclusion

(1) A numerical method, consisting of the recently developed $\overline{c^2} - \varepsilon_c$ model and CFD formulation, is proposed for predicting the concentration and velocity distributions (profiles) of liquid phase as well as the turbulent mass transfer diffusivity in an industrial scale randomly packed distillation column. The advantage of this approach is having avoided introducing the empirical Schmidt number or experimental

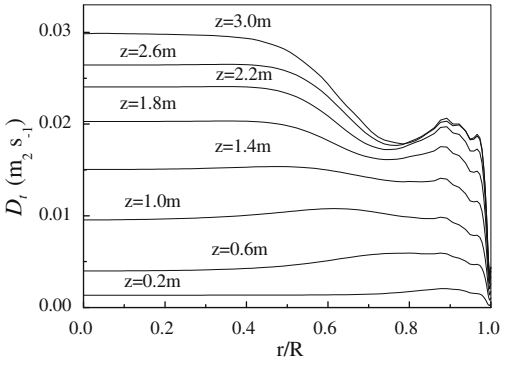

Fig. 8. Profiles of diffusivity at different packed-bed heights for F-factor = 1.02 m s^{-1} (kg m^{-3})$^{0.5}$.

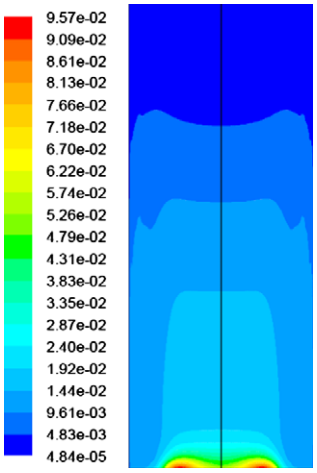

Fig. 9. Contour of turbulent mass transfer diffusivity for *F*-factor = 1.02 m s^{-1} (kg m^{-3})$^{0.5}$.

determined dispersion coefficient. The predicted results agree well with the experimental measurements reported from the literature.

(2) The predicted radial profiles of concentration and velocity in the column display clearly the wall effect due to the non-uniform packed-bed structure and uneven porosity as well as the no-slip boundary at the column wall surface. The shape of radial velocity distribution is consistent with the reported experimental data.

(3) The predicted HETP of the distillation column concerned is in satisfactory agreement with the reported experimental data.

(4) The whole picture on the distribution of dispersion coefficient inside the packed column, which is heavily coupled with the velocity and concentration distribution in the complex turbulent flow and is hardly measured, can be obtained numerically by means of the proposed simulation method.

Acknowledgements

The authors acknowledge the financial support by the National Natural Science Foundation of China (Contract No. 20736005) and the assistance from the staff in the State Key Laboratories for Chemical Engineering (Tianjin University).

Appendix A. Correlations for estimating the parameters in the proposed model

The static holdup H_s for metal Pall rings [31]

$$H_s = 0.033 \exp\left(-0.22 \frac{g\rho}{\sigma a^2}\right)$$

where g is the gravity acceleration constant, σ is liquid surface tension, and a is the surface area per unit volume of packed bed.

The operating holdup H_{op}[32]:

$$H_{op} = 0.555\left(\frac{a\mu^2}{g\gamma^{4.65}}\right)^{1/3}$$

The porosity γ of randomly packed bed [33]:

$$\gamma = \gamma_\infty + \frac{(1-\gamma_\infty)}{2} Er\left\{(1-0.3p_d)\times\cos\left(\frac{2\pi}{c_\gamma + 1.6Er^2}\frac{R-r}{p_d d_p}\right) + 0.3p_d\right\}$$

where γ_∞ is the porosity in an unbounded packing, R is the radius of the column, r is the position in radial direction, Er is the exponential decaying function, which is given by

$$Er = \exp\left[-1.2p_d\left(\frac{R-r}{d_p}\right)^{3/4}\right]$$

where p_d is the period of oscillation normalized by the nominal particle size and $p_d = 0.94 \times (2+1.414)/3$ for Pall rings; c_γ is a constant depending on the ratio of the particle size to column size:

$$c_\gamma = \frac{2R}{n_\gamma p_d d_p} - 1.6\exp\left[-2.4p_d\left(\frac{R}{d_p}\right)^{3/4}\right]$$

where

$$n_\gamma = \mathrm{int}\left\{\frac{2}{1+1.6\exp\left[-2.4p_d(R/d_p)^{3/4}\right]}\frac{R}{p_d d_p}\right\}$$

Mass transfer coefficients [36]:

$$k_L = \left(\frac{4\Phi_L D U_L}{\pi h\gamma\chi}\right)^{0.5}$$

$$k_G = \left(\frac{4\Phi_G D_G U_G}{\pi(\gamma - h\gamma)\chi}\right)^{0.5}$$

$$\frac{a_e}{a} = \frac{h\gamma}{1.0-\gamma}$$

where D_G is the vapor molecular diffusion coefficient, U_L,U_G are the liquid and vapor phase superficial velocities, respectively, the liquid and gas phase enhancement factors Φ_L, Φ_G are equal to unity at the operating conditions concerned. The characteristic length χ for different types of packing can be expressed by:

$$\chi = C_{pk}^2 Z$$

where the dimensionless characteristic constant C_{pk} is equal to 0.031 for 50.8 mm metal Pall rings, Z is the packed-bed height.

Pressure drops Δp_d and Δp_L [34]:

$$\Delta p_d = p_1 G_f^2 \times 10^{p_2 L_f}$$

$$\Delta p_L = 0.774\left(\frac{L_f}{20,000}\right)^{0.1}(p_1 G_f^2 \times 10^{p_2 L_f})^4$$

where $p_1 = 0.04002$, $p_2 = 0.0199$, G_f is the gas loading factor, and L_f is the liquid loading factor. G_f and L_f can be determined by the following correlations:

$$G_f = G(1.2/\rho_G)^{0.5}(F_{pd}/65.62)^{0.5} \quad \text{For } p_t \le 1.0 \text{ atm}$$

$$G_f = G(1.2/\rho_G)^{0.5}(F_{pd}/65.62)^{0.5} \times 10^{0.0187\rho_G} \quad \text{For } p_t > 1.0 \text{ atm}$$

$$L_f = L(1000/\rho)(F_{pd}/65.62)^{0.5}\mu^{0.2} \quad \text{For } F_{pd} \ge 15$$

$$L_f = L(1000/\rho)(65.62/F_{pd})^{0.5}\mu^{0.1} \quad \text{For } F_{pd} < 15$$

The term F_{pd} is a dry packing factor, specified for a given type and size of packing. For 50.8 mm metal Pall rings, $F_{pd} = 79$ m^{-1}.

Body force $\mathbf{F}_{LS}$ [35]:

The liquid flow resistance created by the presence of random packing, the body force, can be calculated by Ergun equation [35]. In this equation, the mean porosity is replaced by the porosity distribution function γ.

$$\mathbf{F}_{LS} = -\left(150\mu\frac{(1-\gamma)^2}{\gamma^2 d_e^2} + 1.75\rho\frac{(1-\gamma)}{\gamma d_e}|\mathbf{u}|\right)\mathbf{u}$$

where the mean porosity γ in this paper is referred to the porosity distribution function, d_e is the equivalent diameter of the random packing, which is defined by

$$d_e = \frac{6(1-\gamma_\infty)}{a}$$

References

[1] B.T. Liu, Study of a new mass transfer model of CFD and its application on distillation tray, Ph.D. Thesis Tianjin University, Tianjin, China, 2003.
[2] A. Shariat, J.G. Kunesh, Packing efficiency testing on a commercial scale with good (and not so good) reflux distribution, Industrial & Engineering Chemistry Research 34 (4) (1995) 1273–1279.
[3] O. Bey, G. Eigenberger, Fluid flow through catalyst filled tubes, Chemical Engineering Science 52 (8) (1997) 1365–1376.
[4] M. Giese, K. Rottschafer, D. Vortmeyer, Measured and modeled superficial flow profiles in packed beds with liquid flow, AIChE Journal 44 (2) (1998) 484–490.
[5] X. Wen, Y. Shu, K. Nandakumar, K.T. Chuang, Predicting liquid flow profile in randomly packed beds from computer simulation, Aiche Journal 47 (8) (2001) 1770–1779.
[6] X.J. Yuan, F.S. Li, K.T. Yu, Distribution of liquid phase in a large packed column, Journal of Chemical Industry & Engineering (China) 40 (6) (1989) 686–692.
[7] Z.T. Zhang, Study on liquid flow characteristics and mass transfer model in packed column, Ph.D. Thesis, Tianjin University, Tianjin, China, 1986.
[8] Z.T. Zhang, K.T. Yu, Stochastic simulation of liquid flow distribution in packed column, Journal of Chemical Industry & Engineering (China) 39 (2) (1988) 162–169.
[9] I. Ziolkowska, D. Ziolkowski, Fluid-flow inside packed-beds, Chemical Engineering and Processing 23 (3) (1988) 137–164.
[10] D.K. Choe, W.L. Lee, Liquid phase dispersion in a packed column with countercurrent two-phase flow, Chemical Engineering Communication 34 (1985) 295–300.
[11] D. Liou, C.S. Tan, Axial dispersion of supercritical carbon dioxide in packed beds, Industrial & Engineering Chemistry Research 28 (8) (1989) 1246–1250.
[12] D. Strang, C. Geankoplis, Longitudinal diffusivity of liquids in packed beds, Industrial & Engineering Chemistry 50 (9) (1958) 1305–1308.
[13] V.P. Dorweiler, R.W. Fahien, Mass transfer at low flow rates in a packed column, AIChE Journal 5 (2) (1959) 139–144.
[14] E.A. Ebach, R. White, Mixing of fluids flowing through beds of packed solids, AIChE Journal 4 (2) (1958) 161–169.
[15] R.W. Fahien, J.M. Smith, Mass transfer in packed beds, AIChE Journal 1 (1) (1955) 28–37.
[16] R.W. Michell, I.A. Furzer, Mixing in trickle flow through packed beds, The Chemical Engineering Journal 4 (1) (1972) 53–63.
[17] T. Otake, E. Kunugita, Mixing characteristics of irrigated packed towers, Journal of Chemical Engineering of Japan 22 (1958) 144.
[18] V.E. Sater, O. Levenspiel, Two-phase flow in packed beds, Industrial & Engineering Chemistry Fundamentals 5 (1) (1966) 86–92.
[19] S.T. Wang, S.Z. Chen, C.L. Li, Methods of estimating axial mixing of liquid phases in packed columns, Chemical Engineering (China) 16 (5) (1988) 46–50.
[20] R. Macias-Salinas, J. Fair, Axial mixing in modern packings, gas, and liquid phases: Ii. Two-phase flow, AIChE Journal 46 (1) (2000) 79–91.
[21] R. Billet, Packed Towers in Processing and Environmental Technology, VCH Publisher, Weinheim, Germany, 1995.
[22] M.J.S. de Lemos, M.S. Mesquita, Turbulent mass transport in saturated rigid porous media, International Communications in Heat and Mass Transfer 30 (1) (2003) 105–113.
[23] F.H. Yin, C.G. Sun, A. Afacan, K. Nandakumar, K.T. Chuang, CFD modeling of mass-transfer processes in randomly packed distillation columns, Industrial & Engineering Chemistry Research 39 (5) (2000) 1369–1380.
[24] Y. Nagano, C. Kim, A 2-equation model for heat-transport in wall turbulent shear flows, Journal of Heat Transfer – Transactions of the ASME 110 (3) (1988) 583–589.
[25] Z.M. Sun, B.T. Liu, X.G. Yuan, C.J. Liu, K.T. Yu, New turbulent model for computational mass transfer and its application to a commercial-scale distillation column, Industrial & Engineering Chemistry Research 44 (12) (2005) 4427–4434.
[26] G.B. Liu, K.T. Yu, X.G. Yuan, C.J. Liu, Q.C. Guo, Simulations of chemical absorption in pilot-scale and industrial-scale packed columns by computational mass transfer, Chemical Engineering Science 61 (19) (2006) 6511–6529.
[27] G.B. Liu, K.T. Yu, X.G. Yuan, C.J. Liu, New model for turbulent mass transfer and its application to the simulations of a pilot-scale randomly packed column for CO_2–NaOH chemical absorption, Industrial & Engineering Chemistry Research 45 (9) (2006) 3220–3229.
[28] Y.S. Zhang, Turbulence National Defense, Industry Press, Beijing, 2002.
[29] A. de Klerk, Voidage variation in packed beds at small column to particle diameter ratio, AIChE Journal 49 (8) (2003) 2022–2029.
[30] L.H.S. Roblee, R.M. Baird, J.W. Tierney, Radial porosity variations in packed beds, AIChE Journal 4 (4) (1958) 460–464.
[31] V. Engel, J. Stichmair, W. Geipel, A new model to predict liquid holdup in packed columns-using data based on capacitance measurement techniques, Instrumentation of Chemical Engineering Symposium Series (1997) 939–947.
[32] J. Stichlmair, J.L. Bravo, J.R. Fair, General model for prediction of pressure drop and capacity of countercurrent gas/liquid packed columns, Gas Separation and Purification 3 (3) (1989) 19–28.
[33] S.J. Liu, A continuum model for gas–liquid flow in packed towers, Chemical Engineering Science 56 (2001) 5945–5953.
[34] L.A. Robbins, Improve pressure-drop prediction with a new correlation, Chemical Engineering Progress 87 (5) (1991) 87–90.
[35] S. Ergun, Fluid flow through packed columns, Chemical Engineering Progress 48 (1952) 89–94.
[36] I. Wagner, J. Stichlmair, J.R. Fair, Mass transfer in beds of modern, high-efficiency random packings, Industrial & Engineering Chemistry Research 36 (1997) 227–237.
[37] E.E. Khalil, D.B. Spalding, J.H. Whitelaw, Calculation of local flow properties in 2-dimensional furnaces, International Journal of Heat and Mass Transfer 18 (6) (1975) 775–791.
[38] R.F. Bird, W.E. Stewart, E.N. Lightfoot, Transport Phenomena, John Wiley & Sons, Inc., New York, 2002.
[39] M. Ferchichi, S. Tavoularis, Scalar probability density function and fine structure in uniformly sheared turbulence, Journal of Fluid Mechanics 461 (2002) 155–182.
[40] S. Tavoularis, S. Corrsin, Experiments in nearly homogeneous turbulent shear-flow with a uniform mean temperature-gradient. 2. The fine-structure, Journal of Fluid Mechanics 104 (MAR) (1981) 349–367.
[41] S. Tavoularis, S. Corrsin, Experiments in nearly homogenous turbulent shear-flow with a uniform mean temperature-gradient, Journal of Fluid Mechanics 104 (MAR) (1981) 311–347.